

Controlling charge transfer in ultracold gases via Feshbach resonances

Marko Gacsa^{1,2} and Robin Côté²

¹NASA Ames Research Center, Moffett Field, CA 94035, USA

²Department of Physics, University of Connecticut, Storrs, CT 06269-3046, USA

(Dated: June 2, 2022)

We investigate the prospects of controlling charge-exchange in ultracold collisions of heteroisotopic combinations of atoms and ions of the same element. The treatment, readily applicable to alkali or alkaline-earth metals, is illustrated in the process ${}^9\text{Be}^+ + {}^{10}\text{Be} \leftrightarrow {}^9\text{Be} + {}^{10}\text{Be}^+$, which exhibits favorable electronic, nuclear, and hyperfine structure. Feshbach resonances are obtained from quantum scattering calculations in a standard coupled-channel formalism with non-BO terms originating from the nuclear kinetic operator. Near a narrow resonance predicted at 322 G, we find the charge-exchange rate coefficient to rise from practically zero to values larger than $10^{-12} \text{ cm}^3/\text{s}$. Our results suggest controllable charge-exchange reactions between different isotopes of suitable atom-ion pairs with potential applications to quantum systems engineered to study charge diffusion in trapped cold atom-ion mixtures and emulate many-body physics.

Since the original studies of ultracold atom-ion scattering [1–3], advances in experimental techniques for direct manipulation of small ensembles composed of ultracold atoms and ions have opened new research venues [4–6]. Production and trapping of cold ions below the critical mass ratio is making possible direct studies of atom-ion collisional dynamics and chemistry at ultracold temperatures [7–11], surpassing the temperature limitations of the experiments in dual overlapping traps for ions and neutrals [12–18]. Of particular interest are applications of such hybrid systems to atom-ion interactions and chemistry [19–23], precision measurements [24], many-body physics [2, 25–31], and quantum information processing [32, 33]. In addition, a number of theoretical proposals suggest different approaches to formation of ultracold molecular ions in their ground state [34–41]. Developing a solid understanding of two-body atom-ion interactions at ultra-low temperatures, and the means to control them *e.g.*, using external electric, magnetic, or optical fields, is central to advancing such research and constitutes an essential step towards envisioning new experiments and developing many-body theoretical descriptions. In atom-ion mixtures, as in neutrals, Feshbach resonances (FRs) are expected to play a key role in controlling the strength and sign of the two-body interaction, consequently altering macroscopic properties of the ensemble [42–44].

First steps to study FRs theoretically in cold atom-ion mixtures have already been undertaken [45–48]. Additionally, near-resonant atom-ion scattering in heteroisotopic mixtures (of H, Be, Li, Rb, and Yb) has been studied theoretically [45, 49, 50, 50–54] where it has been shown that non-Born-Oppenheimer (non-BO) couplings originating from the nuclear kinetic operator influence charge-exchange and scattering cross sections in cold mixtures. This effect is especially significant at ultracold conditions where it could strongly affect the charge diffusion and mobility (see Ref. [2]) with broader consequences for engineered atom-ion systems, such as an ion immersed in a Bose-Einstein condensate (BEC)

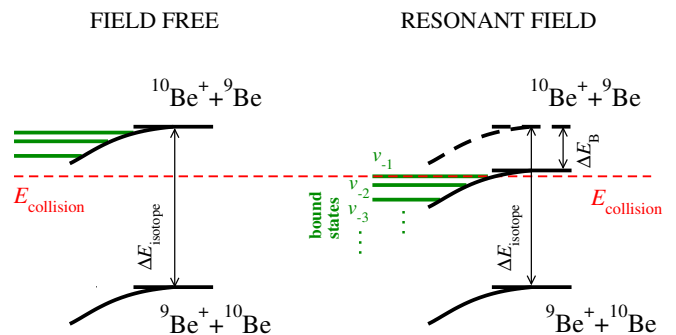


FIG. 1: (Color online) Schematics of the process. *Left*: Field-free scattering for a collision energy $E_{\text{collision}}$ smaller than the asymptotic isotope shift $\Delta E_{\text{isotope}}$. Only the lower asymptote is energetically accessible and charge-exchange to the upper asymptote does not occur. *Right*: The scattering process with a magnetic field B present. The upper asymptote, dressed by B , is shifted down by ΔE_B such that $E_{\text{collision}}$ coincides with a closed channel in the vicinity of a bound state. At specific B fields, charge-exchange can be resonantly enhanced.

[25, 55, 56]. Our choice of heteroisotopic atom-ion pair is motivated by the fact that it is impossible to detect charge-exchange between indistinguishable particles.

In this study, we show that magnetic Feshbach resonances can be used to tune the interparticle interaction to control the resonant charge exchange between different isotopes for selected atom-ion mixtures (Fig. 1). The treatment below applies to systems with one valence electron (*e.g.*, alkali atoms, including H), or one valence hole (*e.g.*, alkaline-earth and some rare earth atoms, like Yb), where at least one of the partners has an hyperfine structure. We note that since both alkaline-earth atoms and ions possess closed optical transitions, it is possible to image them separately, as opposed to alkali species for which ions cannot be optically imaged. Without loss of generality with respect to the choice of species, we select the simplest alkaline-earth element, Be, and study the reaction ${}^9\text{Be} + {}^{10}\text{Be}^+ \rightarrow {}^9\text{Be}^+ + {}^{10}\text{Be}$. For this system, the

molecular ion potential energy curves and their non-BO corrections are known [53] and the isotope energy shift between the two lowest asymptotes suggests that Feshbach resonances will occur at experimentally attainable magnetic fields. Moreover, the fact that ^9Be has a non-zero nuclear spin ($I = 3/2$) and ^{10}Be has zero nuclear spin is suitable for exploring many-body charge dynamics in quantum systems.

If the kinetic energy operator for the center of nuclear mass (CNM) motion is separated out, a collision between an alkaline earth atom and its ion in a magnetic field can be described by an effective Hamiltonian in the body-fixed frame as [43, 57]

$$\hat{H} = \hat{T}_N + \hat{T}_e + \hat{T}_{\text{mp}} + \hat{V}(\vec{r}, \vec{R}) + \hat{H}_{\text{int}} \quad (1)$$

where, \hat{T}_N is the kinetic energy operator describing the relative motion of the nuclei, \hat{T}_e is the electronic kinetic energy operator, $\hat{V}(\vec{r}, \vec{R})$ is the electrostatic interaction operator, \vec{r} are electronic coordinates in the CNM frame, and \vec{R} is the vector connecting the two nuclei. \hat{T}_{mp} is the mass polarization term [53], defined as

$$\hat{T}_{\text{mp}} = -\frac{1}{2m} \sum_{i,j=1}^{N_e} \vec{\nabla}_i \vec{\nabla}_j, \quad (2)$$

where $m = m_1 + m_2$ is the total mass of the nuclei of masses m_1 and m_2 , and the summation runs over the total number of electrons N_e . The operator $\hat{H}_{\text{int}} = \hat{V}_B + \hat{V}_{\text{hf}}$ describes the interactions of the particles' internal degrees of freedom, namely electronic and nuclear spins, in the external magnetic field, $\vec{B} = B\hat{z}$. Specifically, \hat{V}_B can be written as

$$\hat{V}_B = 2\mu_0 B(\hat{S}_{z_1} + \hat{S}_{z_2}) - B \left(\frac{\mu_1}{I_1} \hat{I}_{z_1} + \frac{\mu_2}{I_2} \hat{I}_{z_2} \right), \quad (3)$$

where μ_0 is the Bohr magneton, \hat{S}_{z_i} ($i = 1, 2$) is the z -projection electronic spin operator of the colliding particles, with corresponding nuclear magnetic moment μ_i , nuclear spin quantum number I_i , and z -projection nuclear spin operator \hat{I}_{z_i} . The term \hat{V}_{hf} is given by

$$\hat{V}_{\text{hf}} = \sum_{i=1}^2 \alpha_{\text{hf}}^{(i)} \hat{I}_i \cdot \hat{S}_i, \quad (4)$$

where $\alpha_{\text{hf}}^{(i)}$ is the atomic hyperfine constant ($i = 1, 2$).

The total wave function $\Psi^{J,M}(\vec{r}, \vec{R})$ can be expanded as a sum of partial waves given by the total angular momentum quantum number J and its projection to the internuclear axis M , where, for each (J, M) we have

$$\Psi^{J,M}(\vec{r}, \vec{R}) = e^{iM\varphi} \sum_{\alpha,\Lambda} \frac{1}{R} \chi_{\alpha,\Lambda}^J(R) \Theta_{M,\Lambda}^J(\vartheta) |\alpha\rangle, \quad (5)$$

where Λ is the projection of \vec{L} , the total orbital angular momentum of the electrons, onto the internuclear

axis. The angles of the vector \vec{R} in spherical coordinates are ϑ and φ , $\Theta_{M,\Lambda}^J(\theta)$ is the corresponding generalized spherical harmonic, $\chi_{\alpha,\Lambda}^J(R)$ is the radial wave function describing nuclear motion, and $|\alpha\rangle$ is an eigenstate composed of a BO electronic state and nuclear and electronic spins of the particles. Alkali and alkaline-earth elements have s -state valence electrons (or holes) with no orbital angular momentum ($L_i = 0$), so that $\Lambda = 0$ (since $\vec{L} = \vec{L}_1 + \vec{L}_2 = 0$) and the total spin is $\vec{J} = \vec{I} + \vec{S}$, where $\vec{S} = \vec{S}_1 + \vec{S}_2$ and $\vec{I} = \vec{I}_1 + \vec{I}_2$. In the coupled molecular basis, we can express the state $|\alpha\rangle$ as $|\alpha\rangle = |nJM; SM_S IM_I\rangle$, where n is the ordinal number of the electronic state of the same symmetry, while S and I and the total spin and nuclear spin quantum numbers associated with \vec{S} and \vec{I} , respectively, with their projections onto the internuclear axis given by M_S and M_I . The eigenvalues of the non-relativistic Born-Oppenheimer electronic Hamiltonian, $\hat{H}_{\text{el}} = \hat{T}_e + \hat{V}(\vec{r}, \vec{R})$, for the state $|\alpha\rangle$ are denoted as ε_α .

Since we are primarily interested in dynamics at ultracold conditions, where only the lowest asymptote is energetically accessible, we restrict our analysis to the two energetically lowest electronic states. This approximation is valid for systems whose electronic structure is similar to that of a dimer composed of an alkaline-earth atom and alkaline-earth ion, where a single valent electron (or hole) can participate in the CX process. In addition, we assume s -wave collisions ($J = 0, \Lambda = 0, M = 0$) and neglect higher partial waves. Consequently, we label the two electronic states as $n = 1$ and $n = 2$, respectively. Due to the internal spin degrees of freedom, for each of the electronic states there will exist a total of $N_{\text{hf}} = (2I_1 + 1)(2S_1 + 1)(2I_2 + 1)(2S_2 + 1)$ hyperfine states.

We insert Eq. (5) in the time-independent Schrödinger equation and integrate out the electronic coordinates to obtain a system of coupled-channel equations for the radial wave functions $\chi_\alpha(R)$ at the interaction energy E :

$$\left(-\frac{1}{2\mu} \frac{d^2}{dR^2} + \varepsilon_\alpha - E \right) \chi_\alpha + \sum_{\alpha'} \varepsilon_{\beta\alpha}^{\text{mp}} \chi_{\alpha'} = \frac{1}{\mu} \sum_{\alpha \neq \beta} \langle \beta | \frac{\partial}{\partial R} | \alpha \rangle \frac{d\chi_\alpha}{dR} + \frac{1}{2\mu} \sum_{\alpha} \langle \beta | \frac{\partial^2}{\partial R^2} | \alpha \rangle \chi_\alpha + \sum_{\alpha} \langle \beta | \hat{H}_{\text{int}} | \alpha \rangle \chi_\alpha, \quad (6)$$

where $\mu = (m_9 m_{10}) / (m_9 + m_{10})$ is the reduced mass. We used $m_9 = 9.0121821$ and $m_{10} = 10.013534$ amu. The system can be expressed in a matrix form:

$$\left[\mathbf{I} \frac{d^2}{dR^2} + 2\mathbf{F} \frac{d}{dR} + \mathbf{k}^2 - 2\mu(\mathbf{V} - \mathbf{Z}) \right] \chi = 0 \quad (7)$$

where \mathbf{I} is the identity matrix of dimension $2N_{\text{hf}}$, \mathbf{k}^2 is a diagonal matrix of electronic states' threshold energies

k_j^2 , that satisfy $k_\beta^2 - k_\alpha^2 = 2\mu\Delta E$, where ΔE is the threshold energy. The matrix \mathbf{F} is given by

$$F_{\alpha\beta} = -F_{\beta\alpha} = \langle \alpha | \frac{\partial}{\partial R} | \beta \rangle. \quad (8)$$

The matrix \mathbf{V} originates from the radial and angular part of the nuclear kinetic energy operator, including mass polarization. Its elements are

$$V_{\alpha\beta} = \delta_{\alpha\beta}\varepsilon_\alpha + \varepsilon_{\alpha\beta}^{\text{mp}} + \frac{1}{2\mu} \langle \alpha | \frac{\partial^2}{\partial R^2} | \beta \rangle. \quad (9)$$

The matrix \mathbf{Z} includes the hyperfine and Zeeman interactions given by the last two terms in Eq. (1):

$$Z_{\alpha\beta} = \langle \alpha | (\hat{V}_{\text{hf}} + \hat{V}_B) | \beta \rangle. \quad (10)$$

It is convenient to define a hermitian matrix $\tilde{\mathbf{V}}$ with

$$\tilde{V}_{\alpha\beta} = V_{\alpha\beta} - \frac{1}{2\mu} \frac{d}{dR} F_{\alpha\beta}, \quad (11)$$

and rewrite Eq. (7) so that the proper asymptotic scattering boundary conditions are restored in the atomic representation. The coupled-channel matrix equation is obtained by adding and subtracting two Eqs. (7) and substituting $\tilde{\mathbf{V}}$:

$$\left[\mathbf{I} \frac{d^2}{dR^2} + 2\mathbf{F} \frac{d}{dR} + \mathbf{k}^2 + 2\mu\mathbf{Z} - 2\mu\mathbf{C} \right] \tilde{\chi} = 0, \quad (12)$$

where \mathbf{C} is defined by

$$\begin{aligned} C_{\alpha\alpha} &= \frac{1}{2}(\tilde{V}_{\alpha\alpha} + \tilde{V}_{\beta\beta}) + \tilde{V}_{\alpha\beta} \\ C_{\beta\beta} &= \frac{1}{2}(\tilde{V}_{\alpha\alpha} + \tilde{V}_{\beta\beta}) - \tilde{V}_{\alpha\beta} \\ C_{\alpha\beta} &= \frac{1}{2}(\tilde{V}_{\alpha\alpha} - \tilde{V}_{\beta\beta}) - \frac{d}{dR} F_{\alpha\beta} \\ C_{\beta\alpha} &= \frac{1}{2}(\tilde{V}_{\alpha\alpha} - \tilde{V}_{\beta\beta}) + \frac{d}{dR} F_{\alpha\beta}, \end{aligned} \quad (13)$$

with $\alpha = 1 \dots N_{\text{hf}}$, and $\beta = (N_{\text{hf}} + 1) \dots 2N_{\text{hf}}$.

Let us take a closer look at the matrix elements in Eqs. (8-12). The matrix \mathbf{F} is off-diagonal and contains first derivative couplings between the two electronic states. The diagonal elements of the matrix \mathbf{V} introduce non-BO corrections to ε_α , while its off-diagonal elements couple the two electronic states and asymptotically separate their eigenvalues to the correct limits: $\pm\Delta E/2$. The matrix \mathbf{Z} contains couplings between electronic and nuclear spins and the external magnetic field B . For the non-zero value B , it breaks the degeneracy of hyperfine states' manifolds and splits them into Zeeman sublevels. This phenomenon is responsible for the existence of magnetic Feshbach resonances in diatomic collisions of neutrals [44]. In case of different nuclear spins and different charge arrangements (*i.e.* ${}^9\text{Be}^{10}\text{Be}^+$ vs ${}^{10}\text{Be}^9\text{Be}^+$), in a non-zero B field, the matrix \mathbf{Z} splits each hyperfine

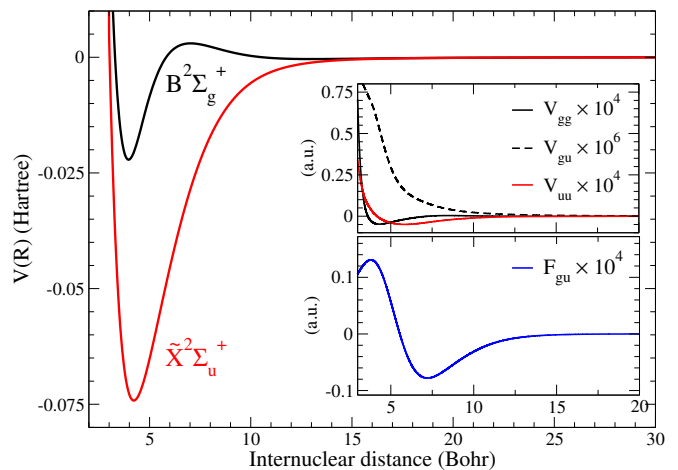


FIG. 2: (Color online) Electronic potentials and non-Born-Oppenheimer couplings for $({}^9\text{Be}^{10}\text{Be})^+$ molecular ion.

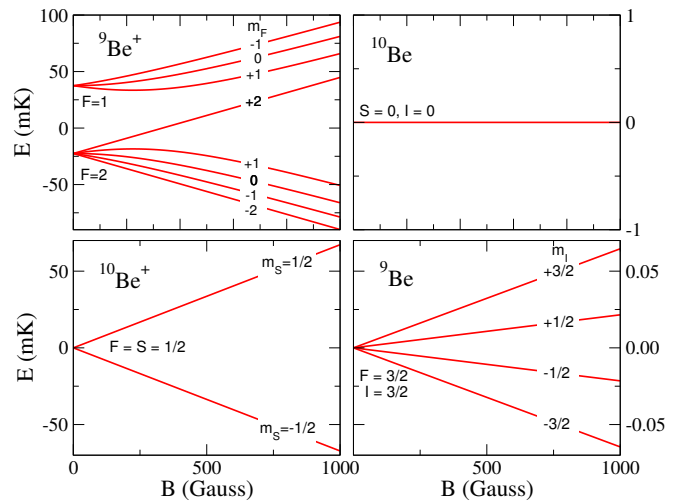


FIG. 3: (Color online) Zeeman splittings of hyperfine states for ${}^9\text{Be}$, ${}^9\text{Be}^+$, ${}^{10}\text{Be}$ and ${}^{10}\text{Be}^+$.

state into Zeeman sublevels that will be coupled if permitted by the symmetry (for $B > 0$ the total projection quantum number $M_F = M_S + M_I$ is conserved and the nuclear spins of two particles are equal, while the total electronic spin $S > 0$). However, the nuclear kinetic operator (matrices \mathbf{F} and \mathbf{V}) will couple individual hyperfine channels as long as the total projection M_F is conserved, giving rise to Feshbach resonances between the states of different asymptotic charge arrangement and leading to magnetically controllable charge exchange.

To illustrate the effects of controlling charge transfer via Feshbach resonances we apply our model to ${}^9\text{Be}^+ + {}^{10}\text{Be}$ in the external magnetic field $\vec{B} = B\hat{z}$. Electronic potential energy curves (PECs) $\tilde{X}^2\Sigma_u^+$ and $B^2\Sigma_g^+$ relevant for this work were studied previously [53, 58, 59], and the effects of the nuclear kinetic operator and isotope shift were calculated [53]. We adopted

the PECs from Ref. [58], the non-BO couplings from Ref. [53], and parametrized the electronic exchange as $V_{\text{exch}}(R) = AR^\alpha e^{-\beta R} (1 + B/R)$, where $A = 0.6316$, $B = -2.72527$, $\alpha = 1.416097$, $\beta = 0.827781$, all in atomic units. We implicitly assumed the uncertainty of the *ab-initio* methods in the exchange region of up to 10% and selected the values that fit Refs. [53] and [58]. The curves were smoothly connected to the long-range form $V_{\text{r}}(R) = \pm V_{\text{exch}}(R) - C_4 R^{-4} - C_6 R^{-6}$ at about $R = 20$ Bohr, where $C_4 = 19.06$ and $C_6 = 274.235$ a.u., and the positive (negative) value of V_{exch} corresponds to $B^2\Sigma_g^+$ ($\tilde{X}^2\Sigma_u^+$), respectively. The final PECs and couplings are given in Fig. 2.

In the external magnetic field the hyperfine states will split into Zeeman sublevels according to the nuclear spins of the Be isotopes: $I = 3/2$ for ^9Be and $I = 0$ for ^{10}Be (Fig. 3). Note that the electronic spin is $S = 0$ for atomic Be and $S = 1/2$ for Be^+ ion. Consequently, there will be $N_{\text{hf}} = 8$ channels for each charge arrangement λ (8×1 for $^9\text{Be}^+ + ^{10}\text{Be}$ (arrangement $\lambda=1$) and 2×4 for $^{10}\text{Be}^+ + ^9\text{Be}$ (arrangement $\lambda=2$) for a total of 16 coupled channels. The channels for which the total M_F is conserved will be coupled, reducing the system size depending on the choice of the entrance channel.

To illustrate the magnetically controlled charge exchange, we select $|1\rangle = |1, -1, 0, 0\rangle_{\lambda=1}$, in the $|F_1, m_{F_1}, F_2, m_{F_2}\rangle_\lambda$ basis, as the entrance channel with the total projection quantum number $M_F = -1$. Here, for $\lambda = 1$, $|F_1, m_{F_1}\rangle$ correspond to $^9\text{Be}^+$, $|F_2, m_{F_2}\rangle$ to ^{10}Be and, for $\lambda = 2$, $|F_1, m_{F_1}\rangle$ to $^{10}\text{Be}^+$, and $|F_2, m_{F_2}\rangle$ to ^9Be . It couples to an open channel $|2\rangle = |2, -1, 0, 0\rangle_{\lambda=1}$ and two closed channels in the upper hyperfine sublevel manifold: $|3\rangle = |\frac{1}{2}, -\frac{1}{2}, \frac{3}{2}, -\frac{1}{2}\rangle_{\lambda=2}$, and $|4\rangle = |\frac{1}{2}, \frac{1}{2}, \frac{3}{2}, -\frac{3}{2}\rangle_{\lambda=2}$, expressed in the same basis. We perform a basis transformation to the $|S, M_S, I, M_I\rangle_\lambda$ basis (see *e.g.* [44, 46]) and solve the Eq. (12) using log-derivative method [60] to calculate the S -matrix and extract the complex scattering length $\eta(B) \equiv a(B) - ib(B)$ in the ultracold limit [44, 61, 62] as a function of the magnetic field for the scattering energy $E = 10 \mu\text{K}$ above the lower asymptote ($\lambda = 1$). The scattering length is shown in Fig. 4 and compared to the asymptotic bound-state model (ABM) [44] with mass-polarization couplings.

For the selected entrance channel, we find four Feshbach resonances caused by the coupling of the entrance channel $|1\rangle$ and closed channel $|3\rangle$. The long-range form of atom-ion potentials, $V(R) \propto -1/R^4$, supports higher density of bound states than the atom-atom interaction, contributing to a larger number of resonances. The broadest resonance occurs at about $B_0 = 322$ G and has a width of $\Delta B = 3$ mG (Fig. 4). We can estimate the charge-exchange cross section $\sigma_{1 \rightarrow 3}^{\text{cx}}$ in the ultracold limit from the expression $\sigma_{1 \rightarrow 3}^{\text{cx}} = \frac{\pi^2}{k^2} (1 - |S_{1,3}|^2) = \frac{4\pi}{k} b$ [2], where $k = \sqrt{2\mu(E - \epsilon_3)}$ and $\epsilon_3(B)$ is the threshold energy for channel $|3\rangle$. For the conditions considered,

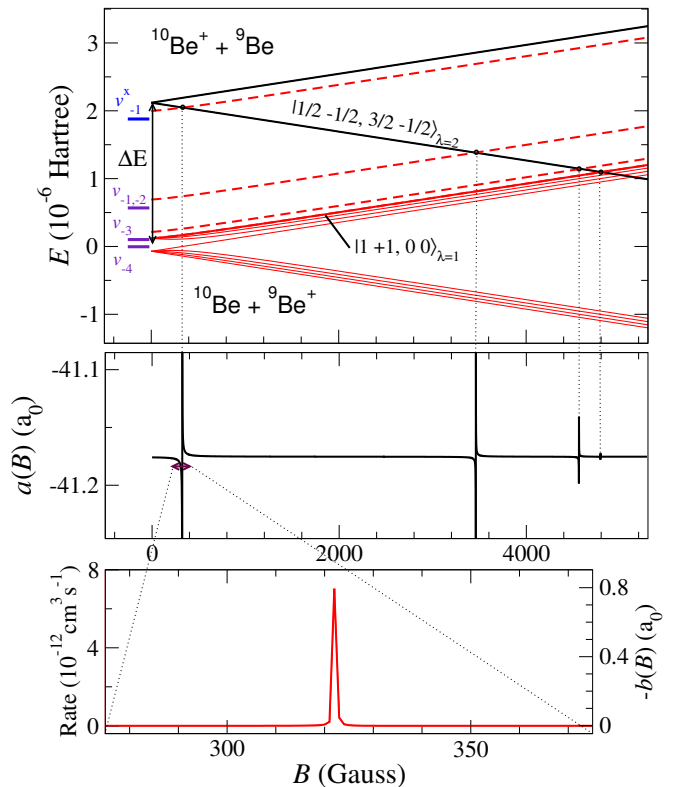


FIG. 4: (Color online) *Top*: Asymptotic model of Feshbach-resonant bound states. Two sets of curves indicate Zeeman-split hyperfine manifolds (for $\lambda = 1$ (red) and $\lambda = 2$ (black)) separated by the isotope shift energy ΔE . Near-dissociation bound vib. levels $v_{-1}(\tilde{X})$ and v_{-1}, \dots, v_{-4} are shown for $\tilde{X}^2\Sigma^+$ (blue) and $B^2\Sigma^+$ (violet) states, respectively, while thick dashed lines (red) correspond to the entrance channel $|1\rangle_{\lambda=1}$ shifted up by their binding energy. The crossings of thick curves indicate magnetic fields for which Feshbach resonances occur. *Middle*: Real part of the scattering length $a(B)$ given as a function of magnetic field B for the entrance channel $|1\rangle$. *Bottom*: Charge-exchange rate as a function of B for the resonance at 322 G.

the CX cross section at $B = B_0$ becomes $\sigma_{1 \rightarrow 3}^{\text{cx}} \approx 10^{-14} \text{ cm}^2$ (for k corresponding to $10 \mu\text{K}$), where we assume $b = -0.02$ a.u. over $\Delta B = 3$ mG. This value compares to the elastic cross section $\sigma^{\text{el}} = 4\pi[a^2 + b^2] \approx 10^{-12} \text{ cm}^2$ for the same assumptions. Therefore, at the Feshbach resonance, about 1% of collisions will result in charge transfer from $^9\text{Be}^+$ to ^{10}Be . The resulting CX rate at ultracold conditions, $K_{\text{cx}}(B) = 4\pi b(B)/\mu$ is given in Fig. 4 (*bottom panel*) for the lowest-field resonance. At the resonance, the CX rate increases from negligible values to about $7 \times 10^{-12} \text{ cm}^3 \text{ s}^{-1}$, indicating that the CX process can be magnetically controlled and experimentally observable rates achieved. Similar results are obtained for higher B -field resonances and for other channels.

In conclusion, we have analyzed atom-ion collisions between $^9\text{Be}^+$ and ^{10}Be in an external magnetic field and shown that weak couplings due to mass polariza-

tion terms can lead to magnetic Feshbach resonances coupling two asymptotically different charge arrangements, ${}^9\text{Be}^+ + {}^{10}\text{Be}$ and ${}^9\text{Be} + {}^{10}\text{Be}^+$, allowing resonant charge transfer. The Feshbach resonances exhibit the usual properties as in neutral systems and, in the analyzed case, allow the charge exchange cross sections to be tuned from zero to about 1% of the value of the elastic cross section. Even though elastic scattering remains the dominant process at ultracold temperatures, the CX rate coefficient can be tuned to significant values of 10^{-12} cm³/s or greater, that are experimentally observable. This is a previously unexplored mechanism of action of Feshbach resonances with possible applications to the studies of charge mobility and diffusion in ultracold gases (see *e.g.*, [2]) and physical systems involving one or more ions in a BEC [15, 25, 56, 63]. The analyzed system likely exhibits a reduction of the resonant coupling strength due to the fact that the $B^2\Sigma^+$ state is weakly repulsive and, at ultracold conditions, prevents the interaction to take place at smaller nuclear separations where the mass-polarization term is stronger. Consequently, Feshbach-resonant charge-exchange cross sections in atom-ion systems with similar electronic configurations, such as $(\text{CaCa})^+$, $(\text{MgMg})^+$ or $(\text{SrSr})^+$, are likely to be larger [59, 64]. The charge-exchange process involving different isotopes can be understood as a chemical reaction with the energy barrier equal to the isotope shift. Therefore, this work is an illustration of a controlled chemical reaction, albeit a trivial one, where it becomes possible to tune the probability for selecting a particular *exit* channel, or a reaction product, via an external magnetic field.

This work was partially supported by the MURI U.S. Army Research Office grant number W911NF-14-1-0378 (MG), and by the PIF program of the National Science Foundation grant number PHY-1415560 (RC). MG was partially supported by an appointment to the NASA Postdoctoral Program at the NASA Ames Research Center, administered by Universities Space Research Association under contract with NASA.

-
- [1] R. Côté and A. Dalgarno, *Phys. Rev. A* **62**, 012709 (2000).
- [2] R. Côté, *Phys. Rev. Lett.* **85**, 5316 (2000).
- [3] O. P. Makarov, R. Côté, H. Michels, and W. W. Smith, *Phys. Rev. A* **67**, 042705 (2003), physics/0209077.
- [4] S. Willitsch, *ArXiv e-prints* (2014), 1401.1699.
- [5] A. Härter and J. Hecker Denschlag, *Contemp. Phys.* **55**, 33 (2014), 1309.5799.
- [6] R. Côté, *Advances in Atomic Molecular and Optical Physics* **65**, 67 (2016).
- [7] T. Huber, A. Lambrecht, J. Schmidt, L. Karpa, and T. Schaetz, *Nat. Commun.* **5**, 5587 (2014), 1408.3269.
- [8] P. Eberle, A. D. Dörfler, C. von Planta, K. Ravi, D. Haas, D. Zhang, S. Y. T. van de Meerakker, and S. Willitsch, *J. Phys. Conf. Ser.* **635**, 012012 (2015).
- [9] S. J. Schowalter, A. J. Dunning, K. Chen, P. Puri, C. Schneider, and E. R. Hudson, *Nat. Commun.* **7**, 12448 (2016), 1608.03376.
- [10] B. Höltkemeier, P. Weckesser, H. López-Carrera, and M. Weidemüller, *Phys. Rev. Lett.* **116**, 233003 (2016), 1505.06909.
- [11] A. Rakshit, C. Ghanmi, H. Berriche, and B. Deb, *J. Phys. B* **49**, 105202 (2016), 1504.03114.
- [12] W. W. Smith, O. P. Makarov, and J. Lin, *J. Mod. Opt.* **52**, 2253 (2005).
- [13] A. T. Grier, M. Cetina, F. Oručević, and V. Vuletić, *Phys. Rev. Lett.* **102**, 223201 (2009), 0808.3620.
- [14] X. Tong, A. H. Winney, and S. Willitsch, *Phys. Rev. Lett.* **105**, 143001 (2010).
- [15] C. Zipkes, S. Palzer, C. Sias, and M. Köhl, *Nature (London)* **464**, 388 (2010), 1002.3304.
- [16] W. G. Rellergert, S. T. Sullivan, S. Kotochigova, A. Petrov, K. Chen, S. J. Schowalter, and E. R. Hudson, *Phys. Rev. Lett.* **107**, 243201 (2011).
- [17] I. Sivarajah, D. S. Goodman, J. E. Wells, F. A. Narducci, and W. W. Smith, *Phys. Rev. A* **86**, 063419 (2012), 1209.2106.
- [18] K. Ravi, S. Lee, A. Sharma, G. Werth, and S. A. Rangwala, *Nat. Commun.* **3**, 1126 (2012).
- [19] P. Blythe, B. Roth, U. Fröhlich, H. Wenz, and S. Schiller, *Phys. Rev. Lett.* **95**, 183002 (2005).
- [20] B. Roth, D. Offenberg, C. B. Zhang, and S. Schiller, *Phys. Rev. A* **78**, 042709 (2008).
- [21] L. Ratschbacher, C. Zipkes, C. Sias, and M. Köhl, *Nat. Phys.* **8**, 649 (2012), 1206.4507.
- [22] S. Haze, R. Saito, M. Fujinaga, and T. Mukaiyama, *Phys. Rev. A* **91**, 032709 (2015), 1403.5091.
- [23] A. Krükov, A. Mohammadi, A. Härter, and J. Hecker Denschlag, *Phys. Rev. A* **94**, 030701 (2016), 1602.01381.
- [24] B. J. Bloom, T. L. Nicholson, J. R. Williams, S. L. Campbell, M. Bishof, X. Zhang, W. Zhang, S. L. Bromley, and J. Ye, *Nature* **506**, 71 (2014), 1309.1137.
- [25] R. Côté, V. Kharchenko, and M. D. Lukin, *Phys. Rev. Lett.* **89**, 093001 (2002), quant-ph/0112113.
- [26] S. Schmid, A. Härter, and J. H. Denschlag, *Phys. Rev. Lett.* **105**, 133202 (2010), 1007.4717.
- [27] R. Gerritsma, A. Negretti, H. Doerk, Z. Idziaszek, T. Calarco, and F. Schmidt-Kaler, *Phys. Rev. Lett.* **109**, 080402 (2012), 1112.3509.
- [28] U. Bissbort, D. Cocks, A. Negretti, Z. Idziaszek, T. Calarco, F. Schmidt-Kaler, W. Hofstetter, and R. Gerritsma, *Phys. Rev. Lett.* **111**, 080501 (2013), 1304.4972.
- [29] J. M. Schurer, P. Schmelcher, and A. Negretti, *Phys. Rev. A* **90**, 033601 (2014), 1407.3575.
- [30] J. M. Schurer, R. Gerritsma, P. Schmelcher, and A. Negretti, *Phys. Rev. A* **93**, 063602 (2016), 1511.00977.
- [31] T. Secker, R. Gerritsma, A. W. Glaetzle, and A. Negretti, *Phys. Rev. A* **94**, 013420 (2016), 1602.04606.
- [32] H. Doerk, Z. Idziaszek, and T. Calarco, *Phys. Rev. A* **81**, 012708 (2010).
- [33] D. J. Wineland and D. Leibfried, *Laser Phys. Lett.* **8**, 188 (2011).
- [34] E. R. Sayfutyarova, A. A. Buchachenko, S. A. Yakovleva, and A. K. Belyaev, *Phys. Rev. A* **87**, 052717 (2013), 1303.3093.
- [35] B. M. McLaughlin, H. D. L. Lamb, I. C. Lane, and J. F. McCann, *J. Phys. B* **47**, 145201 (2014), 1404.6579.
- [36] S. A. Yakovleva, A. K. Belyaev, and A. A. Buchachenko,

- J. Phys. Conf. Ser. **572**, 012009 (2014).
- [37] M. Tomza, C. P. Koch, and R. Moszynski, Phys. Rev. A **91**, 042706 (2015), 1409.1192.
- [38] H. da Silva, Jr., M. Raoult, M. Aymar, and O. Dulieu, New J. Phys. **17**, 045015 (2015), 1501.06385.
- [39] M. Gacesa, J. A. Montgomery, H. H. Michels, and R. Côté, Phys. Rev. A **94**, 013407 (2016), 1603.08032.
- [40] R. Saito, S. Haze, M. Sasakawa, R. Nakai, M. Raoult, H. Da Silva, Jr., O. Dulieu, and T. Mukaiyama, ArXiv e-prints (2016), 1608.07043.
- [41] D. Sardar, S. Naskar, A. Pal, and B. Deb, ArXiv e-prints (2016), 1609.03352.
- [42] W. C. Stwalley, Phys. Rev. Lett. **37**, 1628 (1976).
- [43] T. Kohler, K. Goral, and P. S. Julienne, Rev. Mod. Phys. **78**, 1311 (2006).
- [44] C. Chin, R. Grimm, P. Julienne, and E. Tiesinga, Rev. Mod. Phys. **82**, 1225 (2010).
- [45] B. D. Esry, H. R. Sadeghpour, E. Wells, and I. Ben-Itzhak, J. Phys. B **33**, 5329 (2000).
- [46] Z. Idziaszek, A. Simoni, T. Calarco, and P. S. Julienne, New J. Phys. **13**, 083005 (2011), 1104.5600.
- [47] M. Li, L. You, and B. Gao, Phys. Rev. A **89**, 052704 (2014), 1402.3704.
- [48] M. Tomza, Phys. Rev. A **92**, 062701 (2015), 1509.05390.
- [49] H. R. Sadeghpour, J. L. Bohn, M. J. Cavagnero, B. D. Esry, I. I. Fabrikant, J. H. Macek, and A. R. P. Rau, J. Phys. B **33**, R93 (2000).
- [50] E. Bodo, P. Zhang, and A. Dalgarno, New J. Phys. **10**, 033024 (2008).
- [51] P. Zhang, A. Dalgarno, and R. Côté, Phys. Rev. A **80**, 030703 (2009).
- [52] P. Zhang, E. Bodo, and A. Dalgarno, J. Phys. Chem. A **113**, 15085 (2009).
- [53] P. Zhang, A. Dalgarno, R. Côté, and E. Bodo, Phys. Chem. Chem. Phys. **13**, 19026 (2011).
- [54] T. V. Tscherbul, P. Brumer, and A. A. Buchachenko, Phys. Rev. Lett. **117**, 143201 (2016).
- [55] T. Karpiuk, M. Brewczyk, K. Rzążewski, A. Gaj, J. B. Balewski, A. T. Krupp, M. Schlagmüller, R. Löw, S. Hofferberth, and T. Pfau, New J. Phys. **17**, 053046 (2015).
- [56] J. Wang, M. Gacesa, and R. Côté, Phys. Rev. Lett. **114**, 243003 (2015), 1410.7853.
- [57] A. J. Moerdijk, B. J. Verhaar, and A. Axelsson, Phys. Rev. A **51**, 4852 (1995).
- [58] S. Banerjee, J. N. Byrd, R. Côté, H. H. Michels, and J. A. M. Jr., Chem. Phys. Lett. **496**, 208 (2010).
- [59] H. Li, H. Feng, W. Sun, Y. Zhang, Q. Fan, K. A. Peterson, Y. Xie, and H. F. Schaefer, III, Mol. Phys. **111**, 2292 (2013).
- [60] B. R. Johnson, J. Comput. Phys. **13**, 445 (1973).
- [61] N. F. Mott and H. S. W. Massey, *The Theory of Atomic Collisions* (Oxford University Press, New York, USA, 1987), 3rd ed.
- [62] N. Balakrishnan, V. Kharchenko, R. C. Forrey, and A. Dalgarno, Chem. Phys. Lett. **280**, 5 (1997).
- [63] J. B. Balewski, A. T. Krupp, A. Gaj, D. Peter, H. P. Büchler, R. Löw, S. Hofferberth, and T. Pfau, Nature **502**, 664 (2013).
- [64] S. Banerjee, J. A. Montgomery, J. N. Byrd, H. H. Michels, and R. Côté, Chem. Phys. Lett. **542**, 138 (2012).